Thermalization, Entanglement, Many-body systems, and all that jazz

1. Entanglement within many-body quantum states drives subsystems to thermalization although the full state remain pure and of zero entropy.
2. Closed many-body systems maybe integrable or not, and it is believed that non-integrable systems with very few conserved laws rapidly thermalize, and the mechanism is the "ETH".
3. Information diffusion within many-body systems could be exponentially fast and lead to "scrambling", "butterfly effect" and ...

Entanglement in two coupled kicked rotors

$$
\begin{aligned}
q_1' &= q_1 + p_1' \\
p_1' &= p_1 + \frac{K_1}{2\pi}\sin(2\pi q_1) + \frac{\mathbf{b}}{2\pi}\sin(2\pi(q_1+q_2)) \\
q_2' &= q_2 + p_2' \\
p_2' &= p_2 + \frac{K_2}{2\pi}\sin(2\pi q_2) + \frac{\mathbf{b}}{2\pi}\sin(2\pi(q_1+q_2)).
\end{aligned}
$$

Quantize this to get a Unitary operator $U = (U_1 \otimes U_2)U_{int}(b)$.
What are the entanglement properties of the eigenstates of U?
What connection does it have to classical chaos?

Use $K_1 = 0.1, K_2 = 0.15$. $N = 1/h$.

Left: $N = 15, 20, 25$: spectral avg. entanglement *vs* coupling

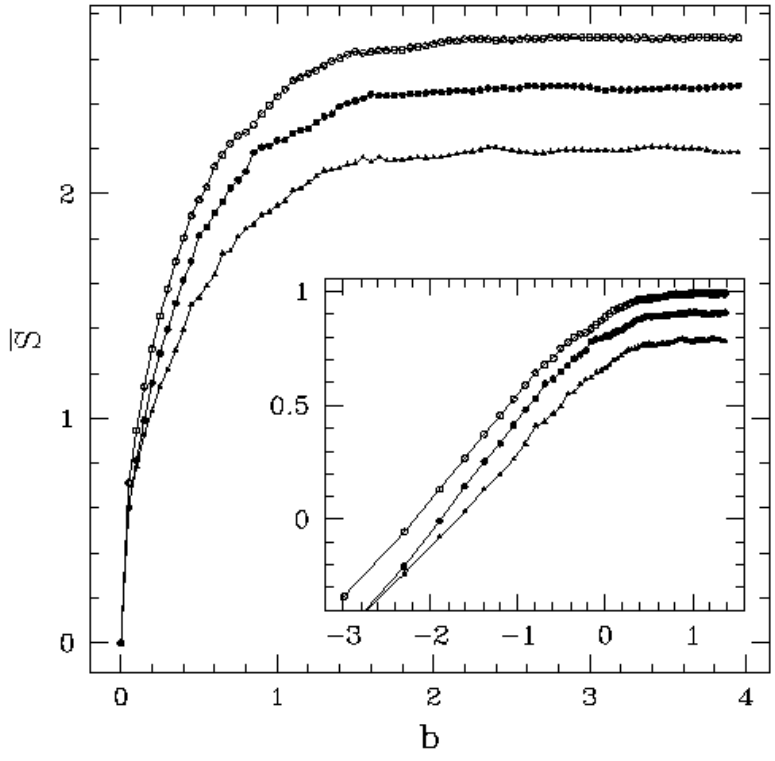

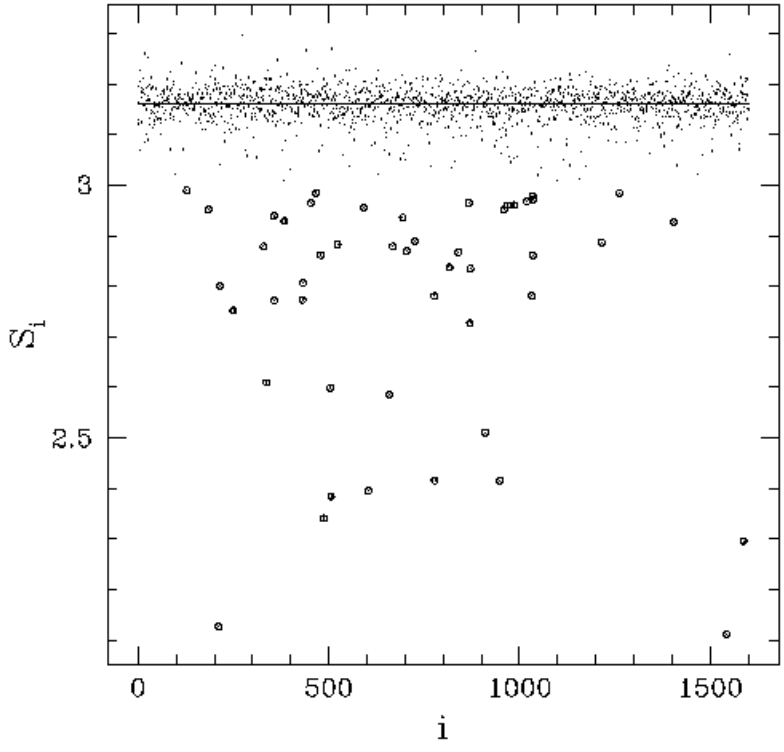

Right: $N = 40, b = 2.0$: Entanglement across a spectrum.

(*Entangling power of quantum chaos*, AL: Phys. Rev. E, 2001)

Two Coupled Quantum Chaotic Tops

QC time evolution leads to near maximum entanglement

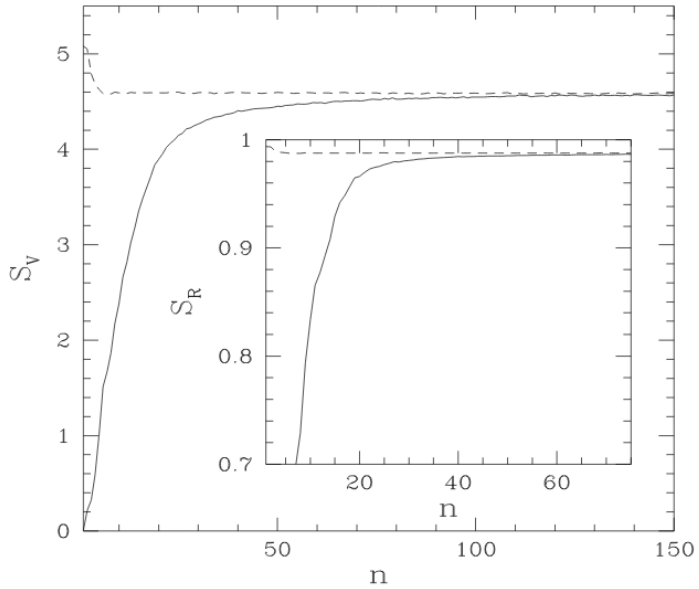

FIG. 1. Entanglement saturation of a completely unentangled initial state (solid line) and a maximally entangled initial state (dotted line) under time evolution operator U_T. Here $k = 3, \epsilon = 0.1$ and the phases $\alpha_1 = \alpha_2 = 0.47$. Inset shows similar behaviour of linear entropy.

Two Coupled Quantum Chaotic Tops

Quantum chaos leads to universal bipartite pure state entanglement: Marcenko-Pastur distribution of eigenvalues of RDM

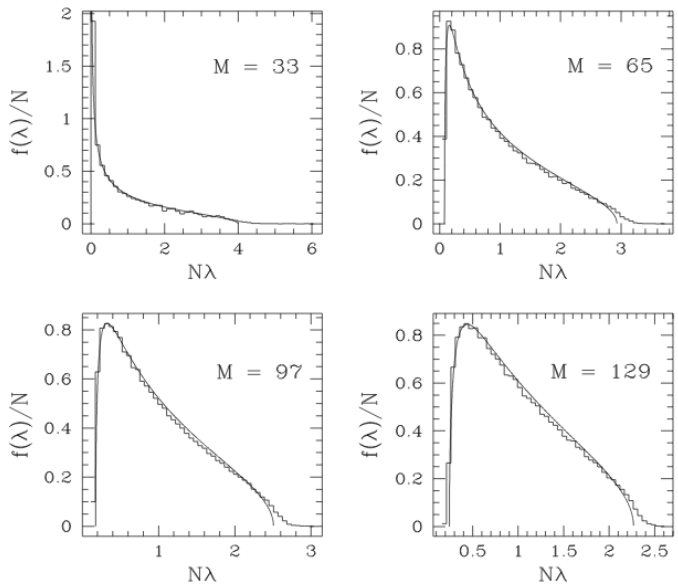

FIG. 3. Distribution of the eigenvalues of the RDMs of coupled kicked tops, averaged over all the eigenstates ($N = 2j_1 + 1 = 33$). Solid curves corresponds to the theoretical distribution function Eq. (7).

The entanglement is nearly maximal and $S = \ln(\gamma N)$. For $N = M$, $S = \ln(N) - 1/2$. As $M \to \infty$, $\gamma \to 1$.
(*J. Bandyopadhyay, AL* Phys. Rev. Lett., 2002)

Ising Model in a tilted magnetic field

$$H(J,B,\theta) = J\sum_{n=1}^{L-1}\sigma_n^z\sigma_{n+1}^z + B\sum_{n=1}^{L}(\sin(\theta)\sigma_n^x + \cos(\theta)\sigma_n^z)$$

Symmetry reduce.

$$\left(\prod_{i=1}^{L}\otimes\sigma_i^y\right)\ H(J,B,\theta)\ \left(\prod_{i=1}^{L}\otimes\sigma_i^y\right)\ =\ -H(-J,B,\theta).$$

$$\mathcal{B}|s_1 s_2 \ldots s_N\rangle = |s_N \ldots s_2 s_1\rangle, \quad [H,\ \mathcal{B}] = 0$$

Quantum Chaos: tilted field . $J = B = 1$

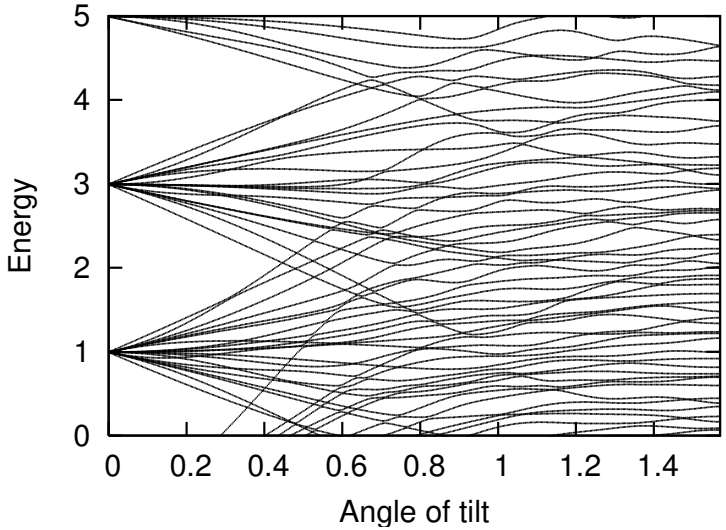

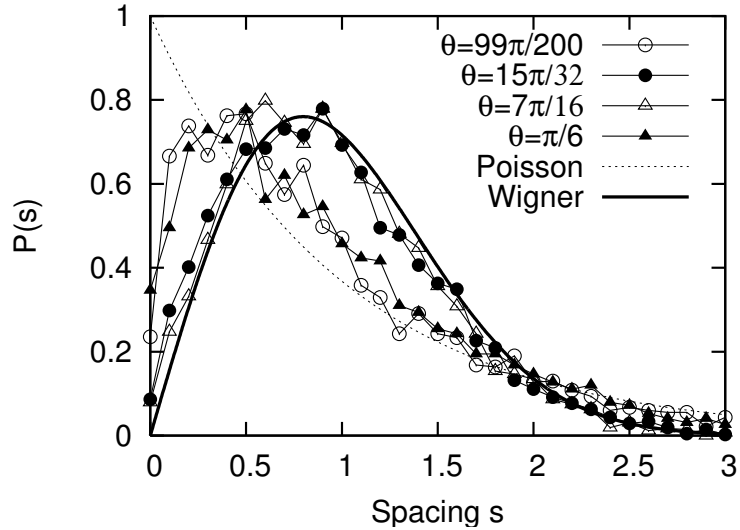

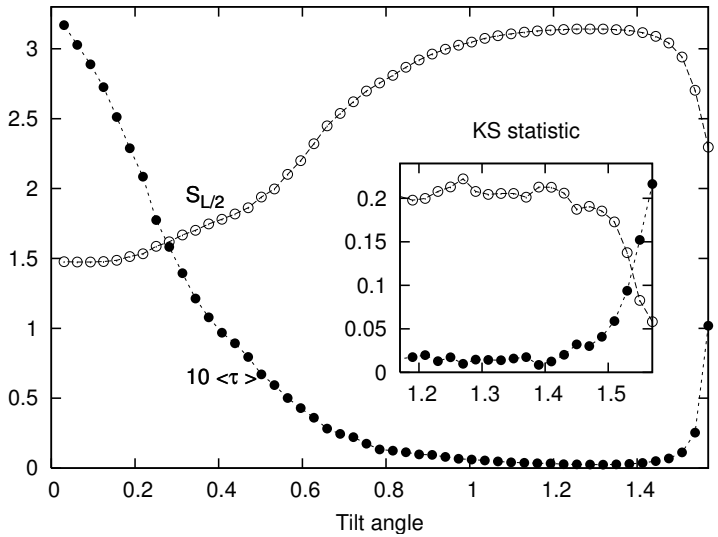

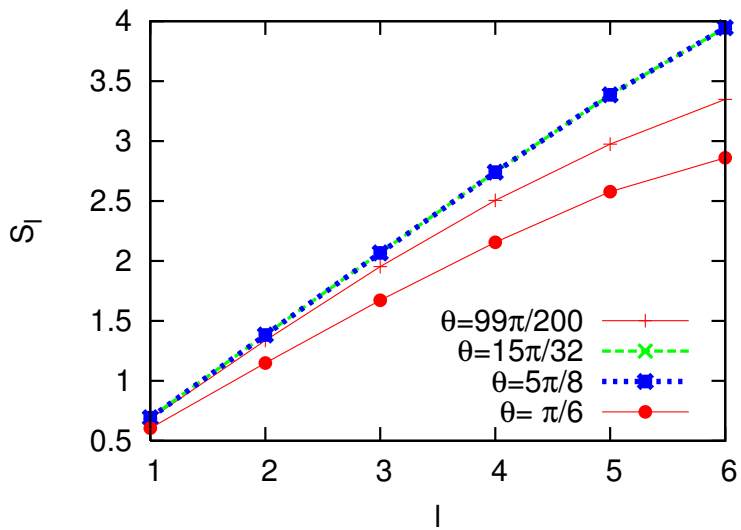

(*J. Karthik, A. Sharma, AL* Phys. Rev. A. (2007))

Spin chains: Many-body localization

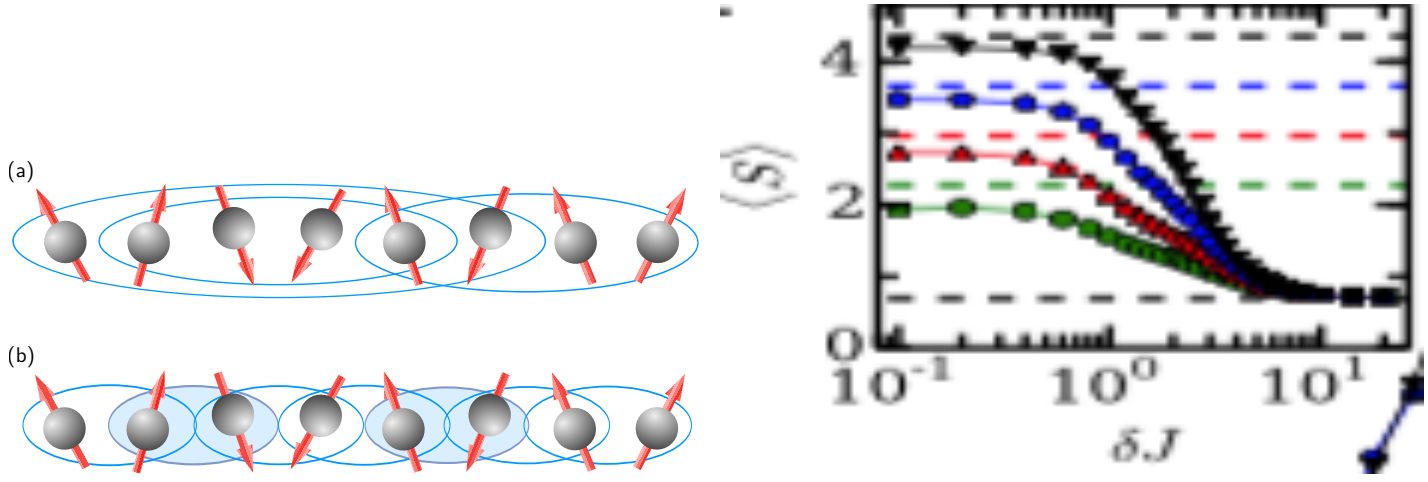

Ising Spins with next nearest neighbor interactions

$$H = -\sum_{i=1}^{L-1} J_i \sigma_i^z \sigma_{i+1}^z + J_2 \sum_{i=1}^{L-2} \sigma_i^z \sigma_{i+2}^z + h \sum_{i=1}^{L} \sigma_i^x$$

(Kjall, Bardarsson, Pollmann, PRL, 2014).

Experiments: 1. Bose Hubbard

to identify fundamental commonalities in the determinants of livelihoods across settings, suggesting that our approach could be used to fill in the large data gaps resulting from poor survey coverage in many African countries. In contrast to other recent approaches that rely on proprietary commercial data sets, our method uses only publicly available data and so is straightforward and nearly costless to scale across countries.

Although our model outperforms other sources of passively collected data (e.g., cellphone data, nightlights) in estimating economic well-being at the cluster level, we are currently unable to assess its ability to discern differences within clusters, as public-domain survey data assign identical coordinates to all households in a given cluster to preserve respondent privacy. In principle, our model can make predictions at any resolution for which daytime satellite imagery is available, though predictions on finer scales would likely be noisier. New sources of ground truth data, whether from more disaggregated surveys or novel crowdsourced channels, could enable evaluation of our model at the household level. Combining our extracted features with other passively collected data, in locations where such data are available, could also increase both household- and cluster-level predictive power.

Given the limited availability of high-resolution time series of daytime imagery, we also have not yet been able to evaluate the ability of our transfer learning approach to predict changes in economic well-being over time at particular locations. Such

STATISTICAL PHYSICS

Quantum thermalization through entanglement in an isolated many-body system

Adam M. Kaufman, M. Eric Tai, Alexander Lukin, Matthew Rispoli, Robert Schittko, Philipp M. Preiss, Markus Greiner*

Statistical mechanics relies on the maximization of entropy in a system at thermal equilibrium. However, an isolated quantum many-body system initialized in a pure state remains pure during Schrödinger evolution, and in this sense it has static, zero entropy. We experimentally studied the emergence of statistical mechanics in a quantum state and observed the fundamental role of quantum entanglement in facilitating this emergence. Microscopy of an evolving quantum system indicates that the full quantum state remains pure, whereas thermalization occurs on a local scale. We directly measured entanglement entropy, which assumes the role of the thermal entropy in thermalization. The entanglement creates local entropy that validates the use of statistical physics for local observables. Our measurements are consistent with the eigenstate thermalization hypothesis.

When an isolated quantum system is perturbed—for instance, owing to a sudden change in the Hamiltonian (a so-called quench)—the ensuing dynamics are determined by an eigenstate distribution that is induced by the quench (*1*). At any given time, the evolving quantum state will have amplitudes that depend on the eigenstates populated by the quench and the energy eigenvalues of the Hamiltonian. In many cases, however,

Department of Physics, Harvard University, Cambridge, MA 02138, USA.
*Corresponding author. Email: greiner@physics.harvard.edu

nag.org/ on January 27, 2018

Experiments: 2. Three globally coupled spins

nature physics

LETTERS

PUBLISHED ONLINE: 11 JULY 2016 | DOI: 10.1038/NPHYS3830

Ergodic dynamics and thermalization in an isolated quantum system

C. Neill[1*†], P. Roushan[2†], M. Fang[1†], Y. Chen[2†], M. Kolodrubetz[3], Z. Chen[1], A. Megrant[2], R. Barends[2], B. Campbell[1], B. Chiaro[1], A. Dunsworth[1], E. Jeffrey[2], J. Kelly[2], J. Mutus[2], P. J. J. O'Malley[1], C. Quintana[1], D. Sank[2], A. Vainsencher[1], J. Wenner[1], T. C. White[2], A. Polkovnikov[3] and J. M. Martinis[1,2]

Statistical mechanics is founded on the assumption that all accessible configurations of a system are equally likely. This requires dynamics that explore all states over time, known as ergodic dynamics. In isolated quantum systems, however, the occurrence of ergodic behaviour has remained an outstanding question[1–4]. Here, we demonstrate ergodic dynamics in a small quantum system consisting of only three superconducting qubits. The qubits undergo a sequence of rotations and interactions and we measure the evolution of the density matrix. Maps of the entanglement entropy show that the full system can act like a reservoir for individual qubits, increasing their entropy through entanglement. Surprisingly, these maps bear a strong resemblance to the phase space dynamics in the classical limit; classically, chaotic motion coincides with higher entanglement entropy. We further show that in regions of high entropy the full multi-qubit system undergoes ergodic dynamics. Our work illustrates how controllable quantum systems can investigate fundamental questions in non-equilibrium thermodynamics.

isolated quantum systems[1–4]. Do quantum systems exhibit ergodic behaviour in the sense of equation (1)? Do quantum systems act as their own bath to approach thermal equilibrium? Extensive experimental efforts have been made to address these fundamental questions[7–13].

Here, we investigate ergodic dynamics by considering a simple quantum model whose classical limit is chaotic[14–18]. This model describes a collection of spin-1/2 particles whose collective motion is equivalent to that of a single larger spin with total angular momentum j governed by the Hamiltonian

$$\mathcal{H}(t) = \frac{\pi}{2\tau} J_y + \frac{\kappa}{2j} J_z^2 \sum_{n=1}^{N} \delta(t - n\tau) \qquad (2)$$

where J_y and J_z are angular momentum operators. The sum over delta functions implies N applications of J_z^2, each at integer time steps. The angular momentum operators can be expressed in terms of the constituent spin-1/2 Pauli operators, for example, $J_z = (\hbar/2)\sum_i \sigma_z^{(i)}$. Setting $\tau = 1$, the first term in $\mathcal{H}$ causes each spin

Kicked tops to many-body spins

$$H = \left(\frac{\hbar p}{\tau}\right) J_y + \left(\frac{\hbar \kappa}{2j}\right) J_z^2 \sum_{n=-\infty}^{\infty} \delta(t - n\tau)$$

(Kus, Scharf, Haake, 1987; Haake's book.)

$J^{x,y,z} = \sum_{l=1}^{2j} \sigma^{x,y,z}/2$, the unitary or Floquet operator:

$$U = \exp\left(-i\frac{\kappa}{8j} \sum_{l \neq l'=1}^{2j} \sigma_l^z \sigma_{l'}^z\right) \exp\left(-i\frac{\pi}{4} \sum_{l=1}^{2j} \sigma_l^y\right),$$

(Wang, Ghose, Sanders, and Hu, 2004)

Thermodynamic limit is also classical limt $j \to \infty$.

Classical Map: $X_n^2 + Y_n^2 + Z_n^2 = 1$

$$X_{n+1} = Z_n \cos(\kappa X_n) + Y_n \sin(\kappa X_n)$$
$$Y_{n+1} = -Z_n \sin(\kappa X_n) + Y_n \cos(\kappa X_n)$$
$$Z_{n+1} = -X_n.$$

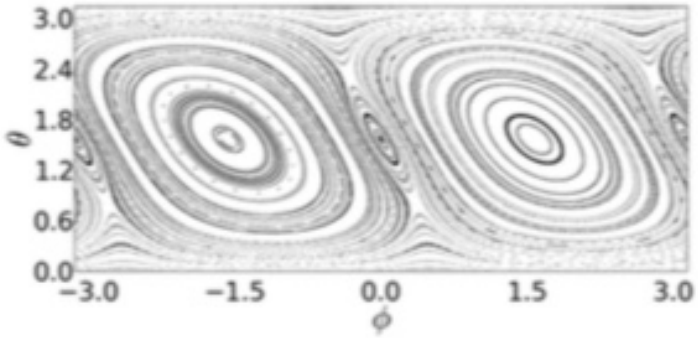

(a)

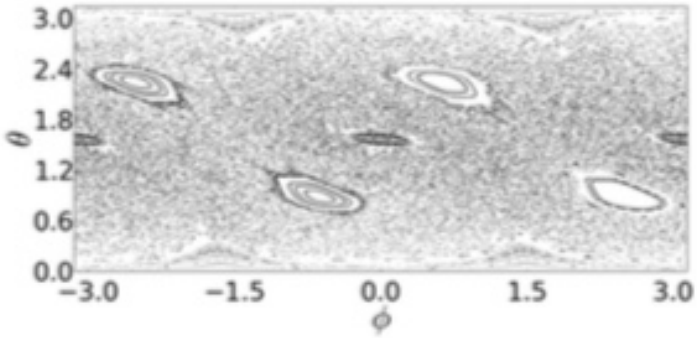

(b)

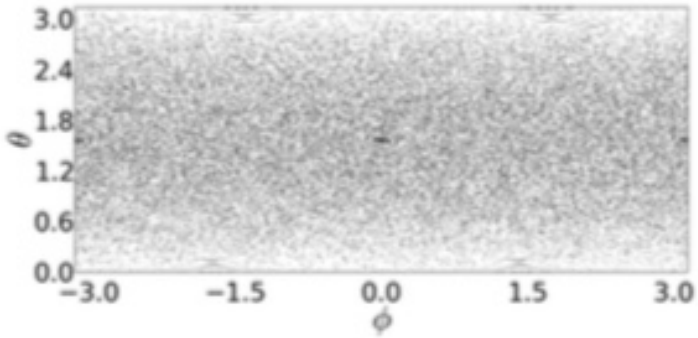

(c)

Results from the 3-Qubit experiment

LETTERS NATURE PHYSICS DOI: 10.1038/NPHYS3830

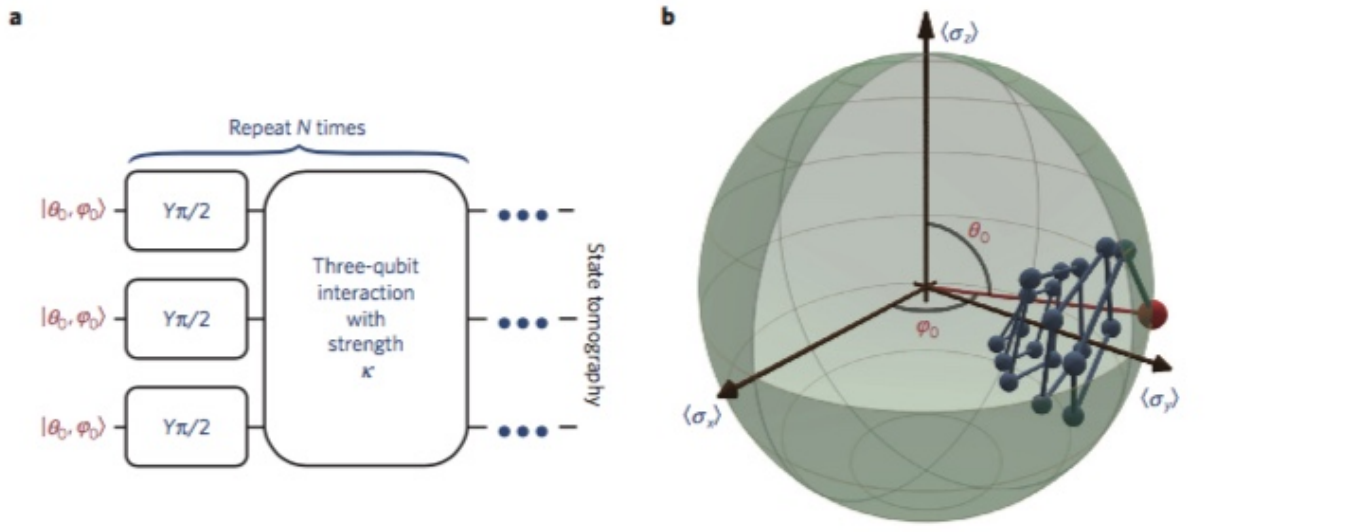

Figure 1 | Pulse sequence and the resulting quantum dynamics. a, Pulse sequence showing first the initial state of the three qubits (equation (4)) followed by the unitary operations for a single time step (equation (3)). These operations are repeated N times before measurement. Single-qubit rotations are generated using shaped microwave pulses in 20 ns; the three-qubit interaction is generated using a tunable coupling circuit controlled using square pulses of length 5 ns for $\kappa = 0.5$ and 25 ns for $\kappa = 2.5$. **b**, The state of a single qubit is measured using state tomography and shown in a Bloch sphere. The initial state is shown in red with subsequent states shown in blue for $N = 1$–20.

Results from the 3-Qubit experiment

NATURE PHYSICS DOI: 10.1038/NPHYS3830 LETTERS

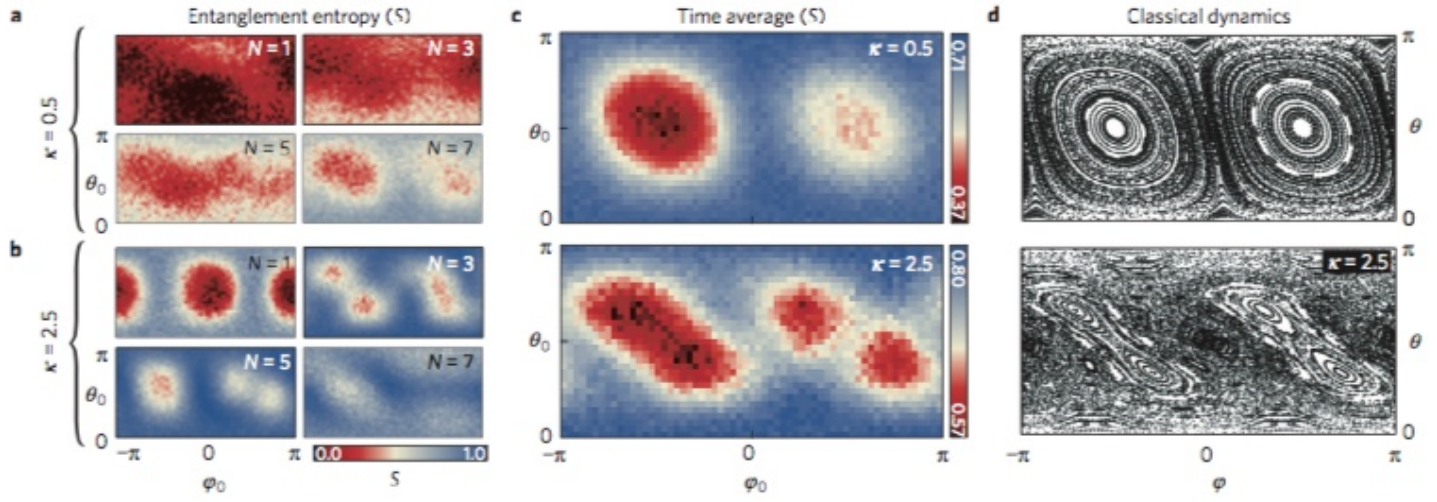

Figure 2 | Entanglement entropy and classical chaos. a,b, The entanglement entropy (colour) of a single qubit (see equation (5)) averaged over qubits and mapped over a 31 × 61 grid of the initial state, for various time steps N and two values of interaction strength $\kappa = 0.5$ (**a**) and $\kappa = 2.5$ (**b**). The entanglement entropy of a single qubit can range from 0 to 1. **c**, The entanglement entropy averaged over 20 steps for $\kappa = 0.5$ and over 10 steps for $\kappa = 2.5$; for both experiments the maximum pulse sequence is ≈500 ns. The left/right asymmetry is the result of experimental imperfections and is not present in numerical simulations (see Supplementary Information). **d**, A stroboscopic map of the classical dynamics is computed numerically and shown for comparison. The map is generated by randomly choosing 5,000 initial states, propagating each state forwards using the classical equations of motion, and plotting the orientation of the state after each step as a point. We observe a clear connection between regions of chaotic behaviour (classical) and high entanglement entropy (quantum).

Results from the 3-Qubit experiment

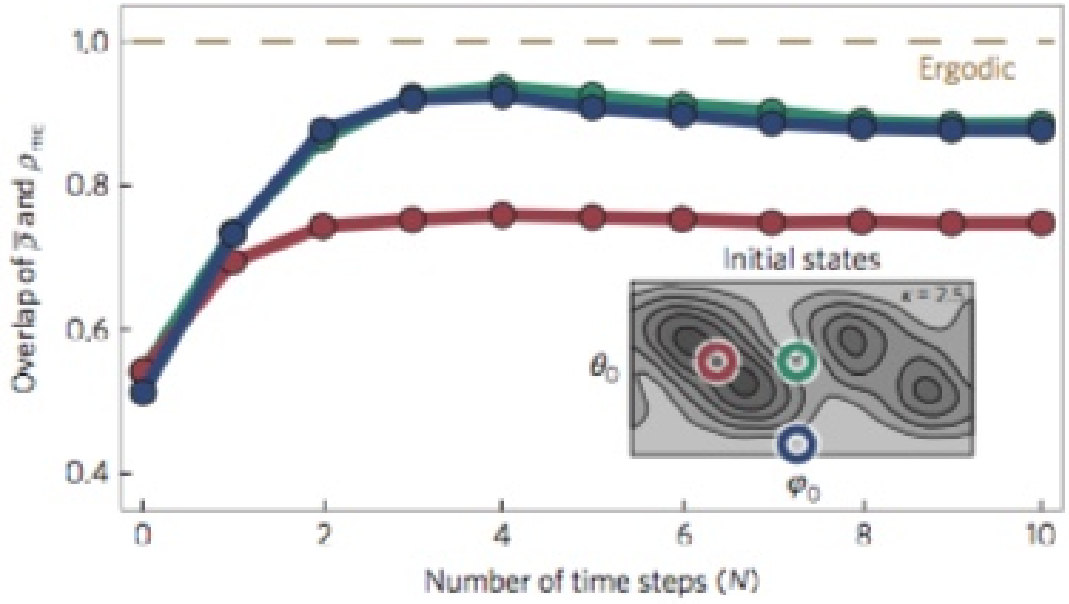

Figure 4 | Ergodic dynamics. The overlap of the time-averaged three-qubit density matrix with a microcanonical ensemble (see equation (6)) versus number of time steps N, for $\kappa = 2.5$. We choose three different initial states, shown inset. A value of 1.0 indicates that the dynamics are fully ergodic.

Eigenstate Thermalization Hypothesis

$$|\psi(t)\rangle = e^{-iHt}|\psi(0)\rangle = \sum_\alpha e^{-iHt}|E_\alpha\rangle\langle E_\alpha|\psi(0)\rangle$$

$$= \sum_\alpha e^{-iE_\alpha t} C_\alpha |E_\alpha\rangle, \quad C_\alpha = \langle E_\alpha|\psi(0)\rangle.$$

$$\rho(t) = |\psi(t)\rangle\langle\psi(t)| = \sum_{\alpha,\beta} e^{-i(E_\alpha - E_\beta)t} C_\alpha C_\beta^* |E_\alpha\rangle\langle E_\beta|$$

$$\overline{\rho(t)} = \sum_\alpha |C_\alpha|^2 |E_\alpha\rangle\langle E_\alpha| \equiv \rho_{diag}$$

$$\overline{A(t)} = \mathrm{Tr}(\rho_{diag} A)? = ?\overline{A_{micro}} = \frac{1}{N_{\Delta E}} \sum_{|E-E_\alpha|<\Delta E} \langle E_\alpha|A|E_\alpha\rangle.$$

ETH: Deutsch, Srednicki, Rigol ...

$$\langle E_\alpha | A | E_\alpha \rangle = \langle A \rangle_{micro, E_\alpha} + \Delta_\alpha .$$

$$\langle \Delta_\alpha \rangle = 0, \langle \Delta_\alpha^2 \rangle \sim \langle A^2 \rangle_{micro} e^{-S(E)}.$$

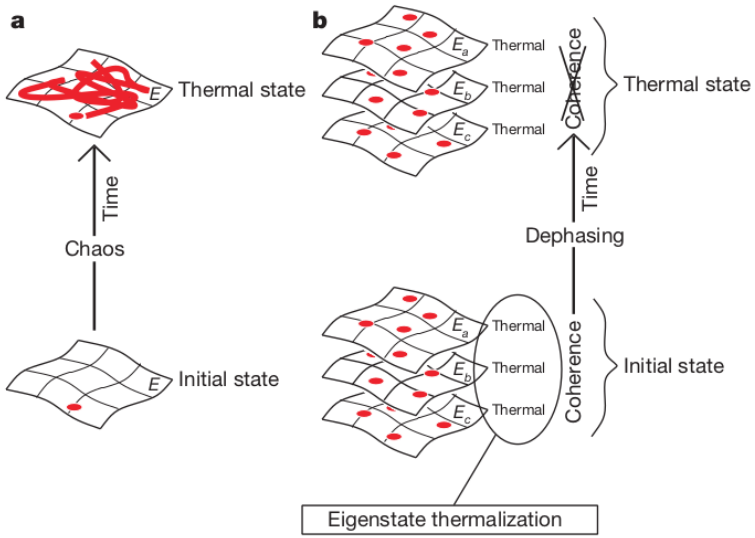

Figure 2 | Thermalization in classical versus quantum mechanics. **a**, In classical mechanics, time evolution constructs the thermal state from an initial state that generally bears no resemblance to the former. **b**, In quantum mechanics, according to the ETH, every eigenstate of the hamiltonian always implicitly contains a thermal state. The coherence between the eigenstates initially hides it, but time dynamics reveals it through dephasing.

(From Rigol et. al., Nature 2008)

ETH: Deutsch, Srednicki, Rigol ...

$$\langle E_\alpha | A | E_\alpha \rangle = \langle A \rangle_{micro, E_\alpha} + \Delta_\alpha .$$

$$\langle \Delta_\alpha \rangle = 0, \langle \Delta_\alpha^2 \rangle \sim \langle A^2 \rangle_{micro} e^{-S(E)}.$$

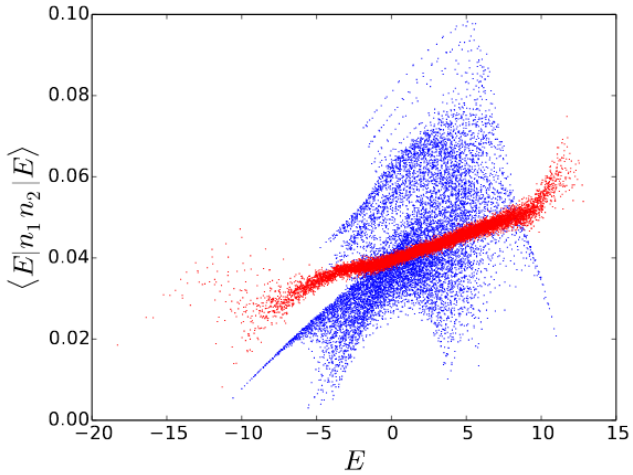

FIG. 6. Numerical results for the hard core boson model of Eq. (18) for 6 particles on 17 lattice sites. The expectation value for the observable $n_1 n_2$, corresponding to the probability that two particles will be next to each other, plotted for different energy eigenstates. The blue points represent the integrable case $V' = t' = 0$, whereas the red points correspond to the non-integrable case $V' = t' = 0.96$

(From J. Deutsch, arXiv:1805.01616)